TECHNION RESEARCH AND DEVELOPMENT FOUNDATION

FINAL TECHNICAL REPORT

Submitted to Air Force Office of Scientific Research, U.S. Air Force

Grant AFOSR - 88 - 0343

Project Title

The Lasing Mechanism of the Orbitron: A Millimeter-Wave Maser Based on a Glow Discharge

Principal Investigator

Prof. Joshua Felsteiner, Department of Physics, Technion - Israel Institute of Technology, Haifa, Israel

October 1992

REPORT DOCUMENTATION PAGE

Form Approved
OMB No. 0704-0188

1. AGENCY USE ONLY (Leave blank)	2. REPORT DATE	3. REPORT TYPE AND DATES COVERED
	October 1992	Final 9/1/88 – 4/30/92

4. TITLE AND SUBTITLE
The Lasing Mechanism of the Orbitron: A Millimeter-Wave Maser Based on a Glow Discharge

5. FUNDING NUMBERS
G: AFOSR-88-0343
PE: 61102F
PR: 2301
TA: D1

6. AUTHOR(S)
Joshua Felsteiner

7. PERFORMING ORGANIZATION NAME(S) AND ADDRESS(ES)
Technion - Israel Institute of Technology
Department of Physics, Technion City, Haifa 32000, Israel

8. PERFORMING ORGANIZATION REPORT NUMBER

9. SPONSORING/MONITORING AGENCY NAME(S) AND ADDRESS(ES)
AFOSR – Bolling AFB, DC 20332 /
EOARD – Box 14, FPO, NY 09510

10. SPONSORING/MONITORING AGENCY REPORT NUMBER
IP 92-01

11. SUPPLEMENTARY NOTES

12a. DISTRIBUTION/AVAILABILITY STATEMENT
Approved for public release;
Distribution unlimited

12b. DISTRIBUTION CODE

13. ABSTRACT (Maximum 200 words)

In this work it was found that the Orbitron microwave generation follows a much stronger generation of RF oscillations close to the ion plasma frequency. This phenomenon is associated with instability of the cathode sheath which causes modulation of the discharge current of almost 100%. These intense RF oscillations are accompanied by short microwave spikes, each emitted at the same phase of the RF period. The microwave radiation has a wide spectrum above the electron plasma frequency. This radiation appears to be due to the transformation of electrostatic plasma waves which were measured inside the plasma and are assumed to be driven by the beam-plasma instability. Both RF and microwave generation do not depend on the anode shape, area, or position.

14. SUBJECT TERMS	15. NUMBER OF PAGES
Microwave & RF Generation; Glow Discharge	28
	16. PRICE CODE

17. SECURITY CLASSIFICATION OF REPORT	18. SECURITY CLASSIFICATION OF THIS PAGE	19. SECURITY CLASSIFICATION OF ABSTRACT	20. LIMITATION OF ABSTRACT
Unclassified	Unclassified	Unclassified	

TR-93-01

This report has been reviewed and is releasable to the National Technical Information Service (NTIS). At NTIS is will be releasable to the general public, including foreign nations.

This technical report has been reviewed and is approved for publication.

PARRIS C. NEAL, Lt Col, USAF
Chief, Aerospace Electronics

RONALD J. LISOWSKI, Lt Col, USAF
Chief Scientist

DTIC

Accession For	
NTIS GRA&I	☑
DTIC TAB	☐
Unannounced	☐
Justification	
By	
Distribution/	
Availability Codes	
Dist	Avail and/or Special
A-1	

TECHNION RESEARCH AND DEVELOPMENT FOUNDATION

FINAL TECHNICAL REPORT

Submitted to Air Force Office of Scientific Research, U.S. Air Force

Grant AFOSR - 88 - 0343

Project Title

The Lasing Mechanism of the Orbitron: A Millimeter-Wave Maser Based on a Glow Discharge

Principal Investigator

Prof. Joshua Felsteiner, Department of Physics, Technion - Israel Institute of Technology, Haifa, Israel

ABSTRACT

In this work it was found that the Orbitron microwave generation follows a much stronger generation of RF oscillations close to the ion plasma frequency ($\omega \lesssim \omega_{p_i}$). The frequency observed was 20 – 70 MHz. This phenomenon is associated with instability of the cathode sheath which causes modulation of the discharge current of almost 100%. These intense RF oscillations are accompanied by short microwave spikes, each emitted at the same phase of the RF period. The microwave radiation has a wide spectrum above the electron plasma frequency ($\omega_{p_e} \lesssim \omega \lesssim 2\omega_{p_e}$). This radiation appears to be due to the transformation of electrostatic plasma waves which were measured inside the plasma and are assumed to be driven by the beam-plasma instability: The beam of primary electrons emitted from the cathode interacts with the discharge plasma. Both the RF generation and the microwave generation do not depend on the anode shape, area, or position.

INTRODUCTION

Current oscillations in glow discharge tubes is a well known phenomenon [1]. Their frequency varies from few Hz to few hundreds of KHz [2], and they are obtained with gas pressures ranging from the sub-Torr regime up to few tens of Torrs. These oscillations are driven mainly by collisional atomic processes: ionization, excitation and recombination. The equations describing these processes are non-linear, leading to sinusoidal oscillations at low currents and chaotic behavior at higher currents [3].

Microwave emission from glow discharge tubes is observed when the gas pressure is low and the discharge current is larger than a certain threshold [4]. Under these conditions the cathode-fall zone becomes narrower than the mean free path of the electrons. Therefore, electrons which are emitted from the cathode and accelerated in the cathode-fall zone gain a kinetic energy equivalent to the cathode-fall voltage. This beam of electrons enters the negative-glow plasma and generates oscillations at frequencies close to the electron plasma frequency, ω_{p_e}. The mechanism is the collisionless beam-plasma instability, which was also investigated with well-controlled beams and plasmas [5].

In 1963 McClure [6] noted 20 MHz oscillations in a low-pressure glow discharge tube, comprising a cylindrical hollow cathode and a very thin coaxial wire anode. This frequency is too high for ionization and recombination processes and much lower than the electron plasma frequency. Neither detailed experimental data nor a theoretical model was provided. Microwave generation in such a tube was reported by Alexeff and Dyer [7]. They attributed this phenomenon to electromagnetic instability of electrons orbiting the positive thin wire anode, and proposed the name "Orbitron" [7,8]. However, a debate arose about this model. Experimental results reported by Schumacher and Harvey [9] and by our group [10] seemed to contradict the Orbitron model. An alternative explanation for the microwave emission was also suggested by Stenzel [11], based on sheath-plasma resonance at the thin-wire anode, which is essentially the monotron instability.

In this report, an experimental study of the low-pressure hollow cathode discharge is presented, that clarifies the situation described above. It was found in this study that above a pressure-dependent threshold current, the tube current was almost 100% modulated at RF frequencies - few tens of MHz. Microwave pulses were radiated at a certain phase of the RF period. Since the anode was a small half sphere located at the end of the cathode cylinder, neither the RF oscillations nor the microwave generation could be attributed to the Orbitron mechanism. Detailed diagnostics of this oscillating discharge tube, which are described later, show that the RF oscillations are driven by a collisionless instability of the ion sheath in the cathode-fall zone. Microwaves are generated from plasma waves, transformed into electromagnetic waves by the plasma inhomogeneity.

THE EXPERIMENTAL SYSTEM

The experimental apparatus is shown in Fig. 1. Two brass open-ended cylinders 4.1 cm and 8.6 cm in diameter, served as cathodes. Both had a length of 10 cm. Initially the anode was a thin coaxial wire, the same as used in the original Orbitrons [7,10]. Later it has been found, in accord with Ref. [9], that the system works in the same way also when the thin wire was moved off axis. Furthermore, it has been found in the present study that the same results are obtained also for an anode in the form of a small coin. This arrangement was more convenient for the purpose of inserting a probe into the tube. Thus the anode was

chosen as a movable brass coin, 5 mm in diameter, which was typically placed at one of the open ends of the cylinder (Fig. 1a). The anode could be moved also to an outside position (Fig. 1b) without any influence on the experimental results. Also the anode area had no influence on the results. The cathode and anode were mounted inside a glass vacuum vessel filled with a gas. Usually He was used but sometimes Ar in order to check the results. The minimum working pressure was 40 – 50 mTorr for the 8.6-cm-diam. tube, and 100 – 150 mTorr for the 4.1-cm-diam. tube. Below these pressures it was impossible to sustain the discharge with the plasma inside the tube, *i.e.* the hollow cathode discharge. The discharge was supported by a pulse current generator built in the following way: An 80-Ω, 2-μs pulse forming network was charged at 3 to 15 kV, and discharged by a thyratron switch into the anode through a 0 to 200 Ω resistor. Typical discharge currents were between 4 and 110 A. A shunt capacitor connected between the anode and the cathode (see Fig. 1) created a low-impedance path for the RF current oscillations. When its capacitance was above a certain value (200 – 250 pF), there was not any significant influence on the instability.

The diagnostics included a Rogowski coil to measure the discharge current, with a very short time resolution (a few ns), and a high resistance divider to measure the pulse voltage across the discharge. The same divider was used for measurements of the plasma potential by a floating single probe. The electron temperature and the spatial distribution of the plasma density were measured by movable double and single Langmuir probes. Comparatively large probes were used (1 mm diameter and 3 mm length) in order to reach a good ion saturation current. Both probes showed the same results. The plasma density n_e is directly proportional to the anode current I_a. Thus, for the 8.6-cm-diam cathode in He in the center of the cathode $n_e \approx 8 \times 10^{10} I_a$ cm^{-3}, and $n_e \approx 2 \times 10^{10} I_a$ cm^{-3} near the walls (3 mm distance). For the 4.1-cm-diam cathode the density increases by 5 – 7 times. The plasma density with Ar is approximately 4 times larger than with He (this was only checked for the 8.6-cm-diam tube). The electron temperature T_e of the main plasma is approximately the same for all diameters and anode currents: $T_e \approx 7 - 8$ eV (He) and $T_e \approx 4.5$ eV (Ar).

In order to analyze the charged particles (electrons and ions) which were going through the cathode sheath, an electrostatic plasma analyzer was mounted

on the cathode surface. Its input grid of 2 cm diameter was a part of the cathode surface (see Fig. 1). By this way one can investigate the potential across the cathode sheath.

Electrostatic plasma waves were probed by a small dipole antenna movable inside the plasma, and radiated microwaves were collected by a horn antenna outside the vacuum vessel. The signals from the antennas were measured by a spectrum analyzer or transferred through a waveguide section to a microwave detector.

RESULTS

The scope traces of the total discharge current I_a, which is slightly below and slightly above the current thresholds, are presented in Figs. 2a and 2b. For both cathode diameters we observed the same current and voltage threshold (but note that the same current corresponds to different densities for the different tube diameters). The RF oscillations appeared to grow up very quickly and the current modulation was about 100%.

The plasma potential V_p and the voltage across the discharge V_a do not depend significantly on the tube diameter and anode postion, but only on the discharge current I_a (see Fig. 3). The difference between V_p and V_a (anode fall) was less than 50 - 60 V in all investigated current range. Also V_p does not depend significantly on the pressure P in this current range. When P changes from 50 to 700 mTorr, V_p changes less than 40 - 50 V. Note that V_p is in fact very close to the cathode fall voltage because it is measured between the cathode and the plasma.

In Fig. 4, the dependence of the generation frequency $\omega_g/2\pi$ of the RF oscillations on the discharge current I_a is presented for both diameters. The frequency increases monotonically with the plasma density n_e independently of whether one increases I_a or decreases the diameter with the same I_a. The period of generation $2\pi/\omega_g$ is of the order of the transit time τ of the ions moving through the cathode sheath. In order to estimate τ we assume the potential drop in the cathode sheath is in accord with the Child-Langmuir law. This assumption is reasonable near the threshold, in which case the cathode sheath is not significantly disturbed yet. Then $\tau \approx 7 - 8$ A, $V \approx 350 - 400$ V, and

taking into account that n_e near the sheath edge is $\sim 0.6n_e$ in the undisturbed plasma, one obtains, with He, $1/\tau \approx 22$ MHz for the 8.6-cm-diam tube and 42 MHz for the 4.1-cm-diam tube. The experimental values are 23 MHz and 30 MHz respectively. With increasing I_a up to 120 A (V_p grows up to 800 V) the difference between $1/\tau$ and $\omega_g/2\pi$ increases by factor 2 - 3. Qualitatively this difference may be explained by pondermotive force due to the RF field in the cathode sheath. This additional force expands the plasma sheath, decreases the ion density in the sheath, and, therefore, reduces ω_g.

In order to check the influence of the ion mass, He was replaced by Ar in the 8.6-cm-diam tube. With the same I_a the density was increased approximately by four times and the ion mass ratio ~ 10. The generation frequency $\omega_g/2\pi$ is decreased by factor 1.4 (see Fig. 4) in good accordance with ion transit time estimates.

The frequency of the RF oscillations does not depend on the pressure P: if P is changed but n_e is kept constant (this is checked by probe), ω_g does not change at all. By increasing the pressure up to a certain value, one can stop the RF generation. The threshold curves for both diameters are presented in Fig. 5. Within the wide pressure range the starting current and voltage are the same for both diameters and do not depend on P. (Of course the density is completely different by factor 5 -7). Increasing P, one can see a sharp edge whose position increases with decreasing diameter. It means that the threshold pressure increases with the density (note that V_p is kept constant). In other words, more exactly, the RF generation breaks when the ratio ν_{in}/ω_g reaches ~ 0.2 - 0.3 independently of the diameter. Here ν_{in} is the ion-neutral collision frequency, $\nu_{in} = v_i \sigma_i N$, $v_i = (2T_i/M)^{1/2}$, $T_i \sim 1$ eV (which is the ordinary value for such plasmas), N is the neutral molecules density, $N = 3.6 \times 10^{16} P(\text{Torr})$, $\sigma_i \approx 4 \times 10^{-15}$ cm^2 is the cross section [12]. Therefore, one can conclude that the growth rate of this instability is $\gamma/\omega_g \gtrsim 0.2$ - 0.3. This value is in good agreement with the scope traces (Fig. 2) where we see a rapid grow up of these oscillations, practically during the formation of the discharge.

Experimental evidence for the strong cathode-fall variation was obtained with the electrostatic charged-particle analyzer which was located at the cathode (see Fig. 1) and which measured separately the ion and electron currents hitting

the cathode. The electrostatic analyzer measurements showed directly a significant changing ($\sim 100\%$) of the cathode fall voltage. The analyzer operated either in ion collecting mode or in electron collecting mode. In Fig. 6a the ion current is presented in absence of RF generation (slightly below the threshold). In Fig. 7a the electron current collected by the analyzer is presented under the same conditions. One can see clearly that the electrons do not penetrate into the cathode sheath if the RF generation does not exist. A completely different picture appears when the RF generation does exist, as is seen in Fig. 6b and 7b for the ion and electron analyzer currents respectively (the discharge current was slightly above the threshold). In Fig. 6c and 7c are shown the same measurements when the discharge current is even higher. From these figures one can see clearly that in certain moments the plasma electrons can penetrate into the cathode sheath up to the cathode wall. It means that in these moments the cathode fall is reduced to very few electron temperatures T_e. Practically it means $\sim 100\%$ reduction because $T_e \ll V_p$. If the AC amplitude is equal to the DC cathode fall voltage, in certain moments the ion current is restricted and the instability stops. This point is supported by the total modulation of the discharge current (Fig. 2). It is noted in Figs. 6b and 6c that the ion current is not totally modulated. This is because of the relatively-long ion transit time.

In Fig. 8 is shown the plasma density spatial distribution as measured by the movable probe for the 8.6-cm-diam tube. The results were the same using a single probe or a double probe. It is seen that the density is maximal near the tube axis and near the anode. The plasma density is of the order of $10^{11} - 10^{12}$ cm^{-3}.

Fig. 9 shows the time evolution of the electrostatic plasma waves spatial distribution, as probed by a small dipole antenna movable inside the 8.6-cm-diam tube. The plasma waves are supposed to be transformed into electromagnetic waves in the microwave range by the plasma inhomogeneity. Fig. 10 shows scope traces of the RF-modulated discharge current along with the detected microwave spikes, each emitted at the same phase of the RF period. Finally, in Fig. 11 is shown an example of the wide spectrum measured by a spectrum analyzer of the microwaves emitted from the 8.6-cm-diam tube for He with a pressure of 70 mTorr. The spectrum is mainly within a certain range above the electron plasma

frequency, $\omega_{p_e} \lesssim \omega \lesssim 2\omega_{p_e}$. It should be noted that due the wide distribution of plasma densities (Fig. 8) the electron plasma frequency also has a wide range, $\omega_{p_e} = (4\pi e^2 n/m)^{1/2}$. The plasma density n depends on the discharge current I_a and can be written as: $n = AI_a$ where A is a geometrical factor which depends on the tube diameter and on the location inside the tube.

DISCUSSION

The RF oscillations cannot be caused by ionization and de-ionization processes because: 1. There was not any frequency dependence on the pressure in the investigated range. 2. Estimation shows that the decay time is too long. Naturally, even if the recombination coefficient β is $\sim 10^{-7}$ cm^3/s [12], the decay time τ is much larger than the oscillation period: $\tau = (\beta n_e)^{-1}$, $(n_e)_{max} \approx 5 \times 10^{13}$ cm^{-3} (for the 4.1-cm-diam tube and $I_a = 100$ A), $\tau_{min} \gtrsim 200$ ns. But the observed value is $2\pi/\omega_g \approx 20$ ns under the same conditions.

In principle, such RF oscillations can also directly occur due to some kind of beam-plasma instability in the plasma body: in fact, there is the beam of the emitted electrons near the cathode sheath (its energy $\sim V_p \gg T_e$). But such an electron flux can cause high frequency oscillations only, $\omega \sim \omega_{p_e}$, where ω_{p_e} is the electron plasma frequency. However, the observed value is $\omega \sim \omega_{p_i}$, where ω_{p_i} is the ion plasma frequency.

As noted before, the anode position and its area have no influence on the RF generation. Therefore, the electron current near the anode also cannot cause this instability.

The cathode sheath disappearance could be caused by strong electron emission. In this case the ion space charge would be compensated by the emitted electron space charge. The condition for this is [13]: $I_e \gtrsim (M/m)^{1/2} I_i$, where I_e is the emitted electron current from the cathode and I_i is the ion current from the plasma. But in the present case $I_e = \alpha I_i$; here $\alpha = 0.1 - 0.5$ [12] (α is the secondary emission coefficient, and $\alpha \ll (M/m)^{1/2}$).

For a possible explanation of the RF experimental results one should take into account the dynamic aspects of the cathode sheath formation. As is well known, the plasma-sheath system near a negative wall reaches a stable structure when the ions arrive at the sheath edge with energies $W_i \geq \frac{1}{2}T_e$ (the Bohm

criterion [14]). This condition defines the state of the sheath with a certain thickness, voltage fall, and charge and electric field distributions. Now suppose that due to some reasons this balanced state is disturbed. This may be due to electron-temperature changing in the plasma body or to space-charge disturbance inside the sheath. Note that the timing of the sheath reaction is determined by the motion of the massive ions. It is possible that the sheath reaction to the electron-temperature changing may create a positive feedback which in turn will lead to sheath instability. This electron-temperature changing may be caused via the beam-plasma instability by the emitted electrons going through the cathode fall into the plasma. Typical times for T_e changing are few $2\pi/\omega_{p_e}$ which are much smaller than the ionic response time $2\pi/\omega_{p_i}$, and hence the ionic response time should determine the frequency of oscillation. Alternatively, the balanced space-charge distribution may be disturbed due to ion flux bunching inside the sheath. In this case, the interaction of the bunched flux with the electric field inside the sheath may create an instability like in conventional microwave electron tubes [15]. However, the large variations in the sheath voltage and in turn the variations in the sheath thickness complicates the analysis of this phenomenon. In any case, both possibilities lead to the same period of oscillations, which is close to the ion transit time through the sheath.

The microwave radiation that is emitted from the discharge (Figs. 10,11) appears to be due to the transformation of plasma waves which were measured inside the plasma (Fig. 9). The beam of primary electrons emitted from the cathode interacts with the discharge plasma. If the velocity of the beam electrons is high enough to overcome the Landau damping mechanism then they will lead to a beam-plasma instabilty. This instability will cause the formation of electrostatic plasma waves. Since the cathode-fall voltage undergoes RF oscillations, the plasma waves will be modulated with the same frequency. This, in turn, will cause the RF modulation of the microwaves [Fig. 10]. The idea that the emitted microwaves are due to plasma waves created inside the plasma has already been mentioned briefly by Schumacher and Harvey [9] who opposed the Orbitron interpretation of Alexeff and Dyer [7,8]. This latter interpretation depends on the existence of a thin wire anode, and attributes the microwave generation to an electromagnetic instability of the electrons orbiting the thin positive wire.

However, in the present study it was found that the results remain the same even if one uses a small coin-shaped anode. Also in the present study the microwave spectrum was found to be rather wide (Fig. 11) while Alexeff and Dyer [7,8] expect, and sometimes claim to observe, narrow peaks. Perhaps some of their experimental conditions were different from the present study, and they relate to a different effect, but they do not give sufficient experimental details to allow a detailed comparison.

Another interpretation of the Orbitron microwave emission was given earlier by the present group [10], using the idea of stimulated emission of bremsstrahlung. This mechanism depends on the existence of collisions in the plasma and therefore should be a function of the gas pressure. However, only later, after the present project has started, better instrumentation has become available to the present group. This has allowed a much better time resolution which, in turn, has lead to the observation of the RF oscillations not seen before. From the threshold curves (Fig. 5) it is seen that at low pressures the effect is pressure independent. Also the beam-plasma instability is a collisionless mechanism. Finally, another alternative explanation for the microwave emission was suggested by Stenzel [11], based on sheath-plasma resonance near the positive thin-wire anode. However, this idea is inconsistent with the present experimental observation that the anode, made also in the form of a coin, could be placed even outside the cylinder (Fig. 1) without changing the experimental results.

CONCLUSIONS

The purpose of the present project was to investigate the microwave emission mechanism of the Orbitron device. Out of several possible interpretations, the present study supports the contention that the beam-plasma instability produces plasma waves which transform into microwaves due to the plasma inhomogeneity. The microwave emission was found to have a rather wide spectrum above the electron plasma frequency. This microwave emission was found to be only a secondary effect to a much stronger effect of RF generation due to a new kind of instability in the hollow cathode discharge. It was shown to be a collisionless instability of the cathode sheath, effecting a large reduction of the sheath voltage and almost 100% modulation of the discharge current. The oscillation frequencies,

which are in the RF regime ($\sim$ 10 MHz - 100 MHz), are related to the ion transit time through the sheath. The present device consists of a very simple and small apparatus, which is magnetic-field free. It was found to produce an output of RF oscillations at a power of the order of 10 kW in a yet unoptimized device. The microwave emission, on the other hand, is only a low-power secondary effect, as only part of the plasma waves transform into electromagnetic waves. In addition, the emitted microwave radiation is strongly modulated by the RF oscillations.

PUBLICATIONS AND CONFERENCES

The results of this investigation will be presented in a contributed paper in the 34th Annual Meeting of the Division of Plasma Physics of the American Physical Society, to be held in Seattle, WA, on 16-20 November, 1992. The abstract of this contribution was published in the Bulletin of the American Physical Society **37**, 1460 (1992), "RF Oscillations and Microwave Generation in a Low-Pressure Hollow Cathode Discharge", and a copy of it is attached to this report. An article describing the results of the present study is being prepared and will be submitted for publication in the Phy ical Review. As a by product, a theoretical investigation was carried out by the present group on the validity of the Orbitron model compared to other related effects. This was published in the Journal of Applied Physics **68**, 5981 (1990), "Collision-Induced Resonant Amplification of Electromagnetic Waves by Electrons in Circular Orbits", and a copy of it is also attached to this report.

REFERENCES

[1] G. Francis, Handbuch der Physik, Band 22, edited by S. Flugge (Springer-Verlag, Berlin, 1957).

[2] A. Balazaras, P. Serapinas, and P. Šimkus, J. Phys. D**18**, 1353 (1985).

[3] T. Braun, J. A. Lisboa, R. E. Francke, and J. A. C. Gallas, Phys. Rev. Lett. **59**, 613 (1987); T. Braun, J. A. Lisboa, and J. A. C. Gallas, Phys. Rev. Lett. **68**, 2770 (1992).

[4] Z. qi Yu, J. J. Rocca, G. J. Collins, J. Appl. Phys. **54**, 131 (1983).

[5] D. A. Whelan and R. L. Stenzel, Phys. Rev. Lett. **50**, 1133 (1983); Phys. Fluids **28**, 958 (1985).

[6] G. W. McClure, Appl. Phys. Lett. **2**, 233 (1963).

[7] I. Alexeff and F. Dyer, Phys. Rev. Lett. **45**, 351 (1980).

[8] I. Alexeff, Phys. Fluids **28**, 1990 (1985).

[9] R. W. Schumacher and R. J. Harvey, Bull. Am. Phys. Soc. **29**, 1179 (1984); 1984 IEEE Int. Conf. on Plasma Science (IEEE, New York, 1984), p. 109.

[10] J. Felsteiner, A. Rosenberg, D. Arbel, and J. Politch, Int. J. Infrared & Millimeter Waves **8**, 479 (1987).

[11] R. L. Stenzel, Phys. Rev. Lett. **60**, 704 (1988).

[12] E. W. McDaniel, *Collision Phenomenoa in Ionized Gases* (Wiley, New York, 1964).

[13] P. D. Prewett and J. E. Allen, Proc. R. Soc. London A**348**, 435 (1976).

[14] K. -U. Riemann, J. Phys. D: Appl. Phys. **24**, 493 (1991).

[15] C. U. Birdsall and W. B. Bridges, *Electron Dynamics of Diode Regions* (Academic, New York, 1966), Chaps. 1,2.

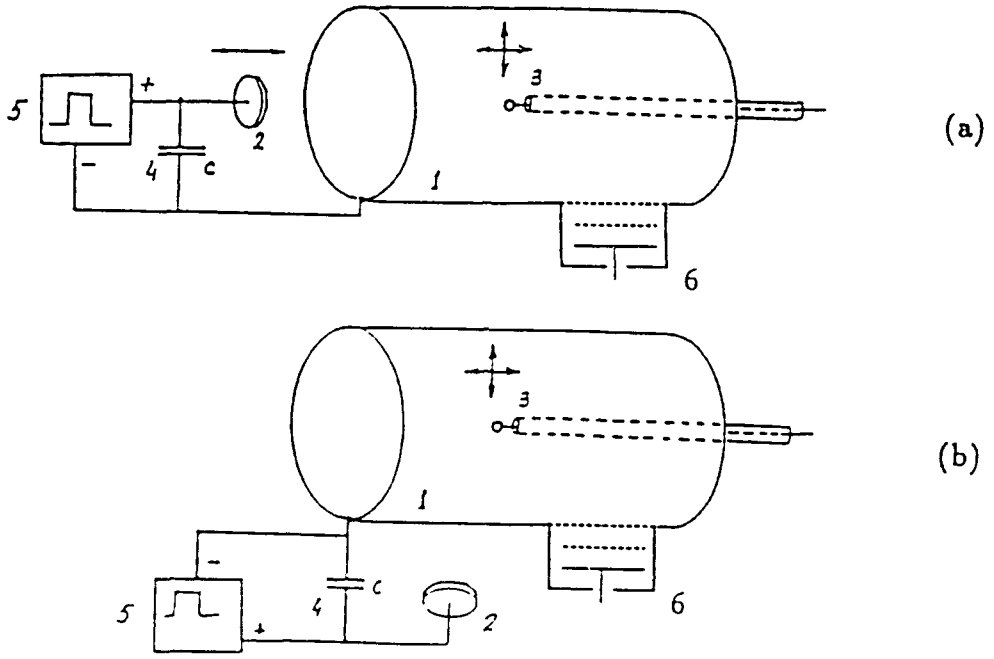

FIG. 1. Experimental apparatus. (a) and (b) refer to different anode locations. 1 – cathode cylinder with 8.6 or 4.1 cm diameter; 2 – anode; 3 – movable probe; 4 – shunt capacitor; 5 – pulse generator; 6 – electrostatic analyzer.

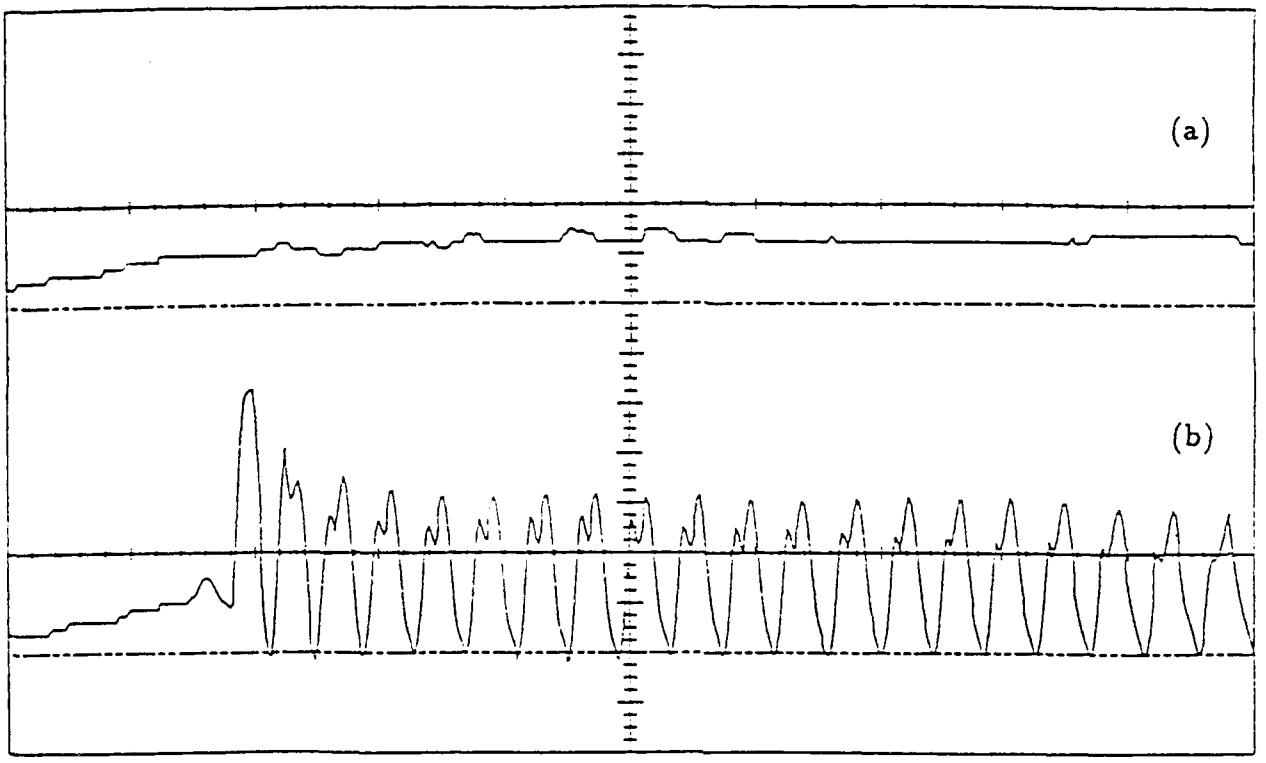

FIG. 2. Scope traces of discharge current. (a) without RF generation; (b) with RF generation. Timebase 100 ns/div, sensitivity 4 A/div. The broken lines show the zero level.

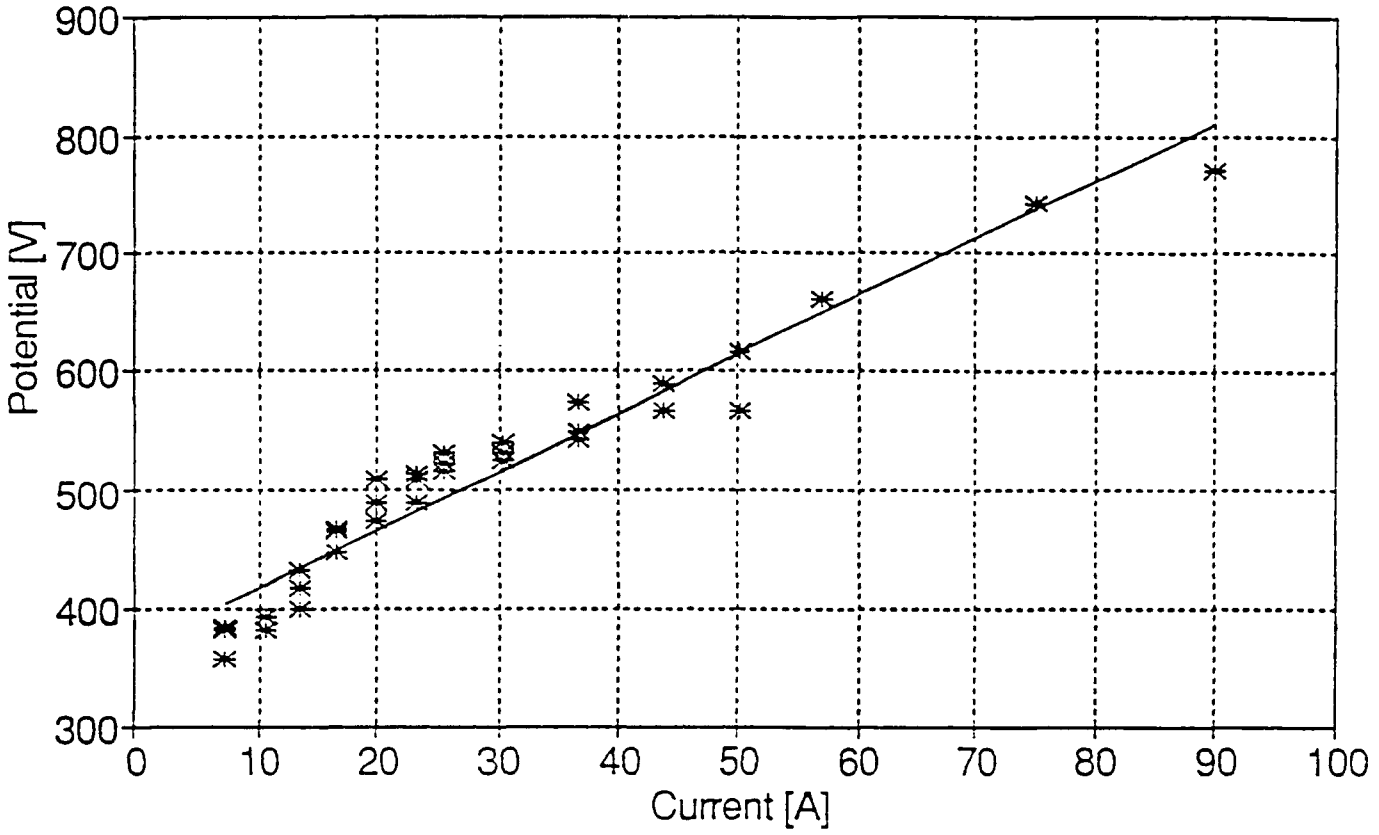

FIG. 3. Floating potential *vs* discharge current.

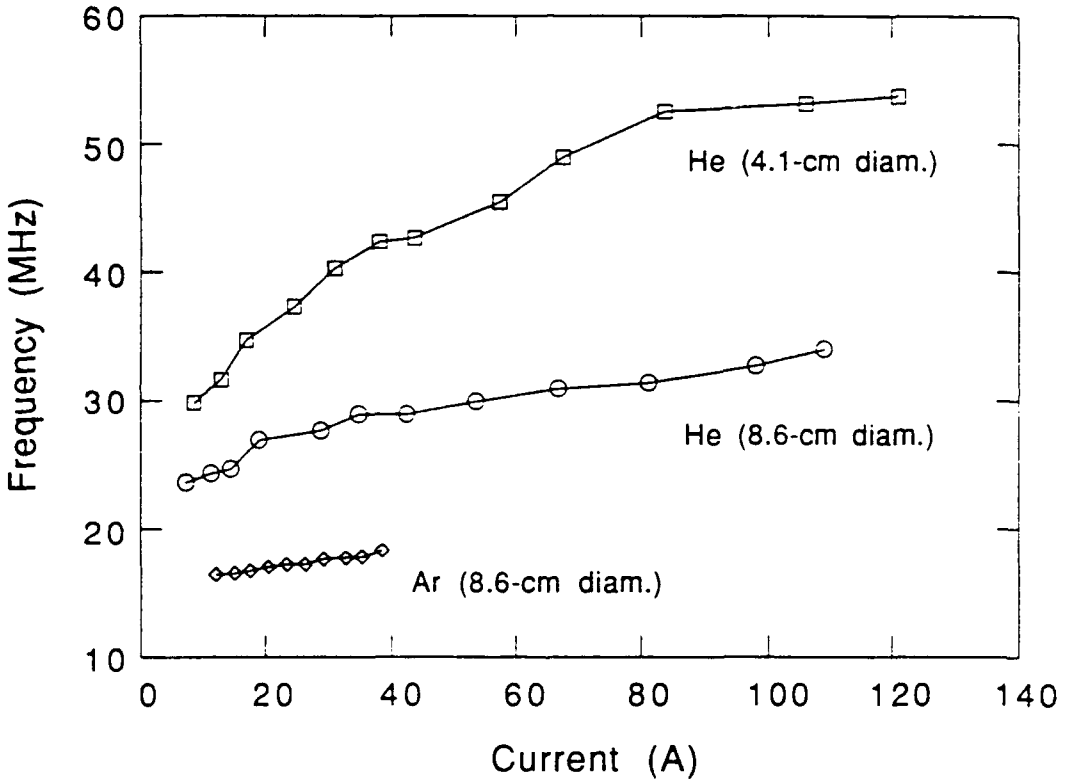

FIG. 4. Frequency dependence of the RF oscillations on the discharge current.

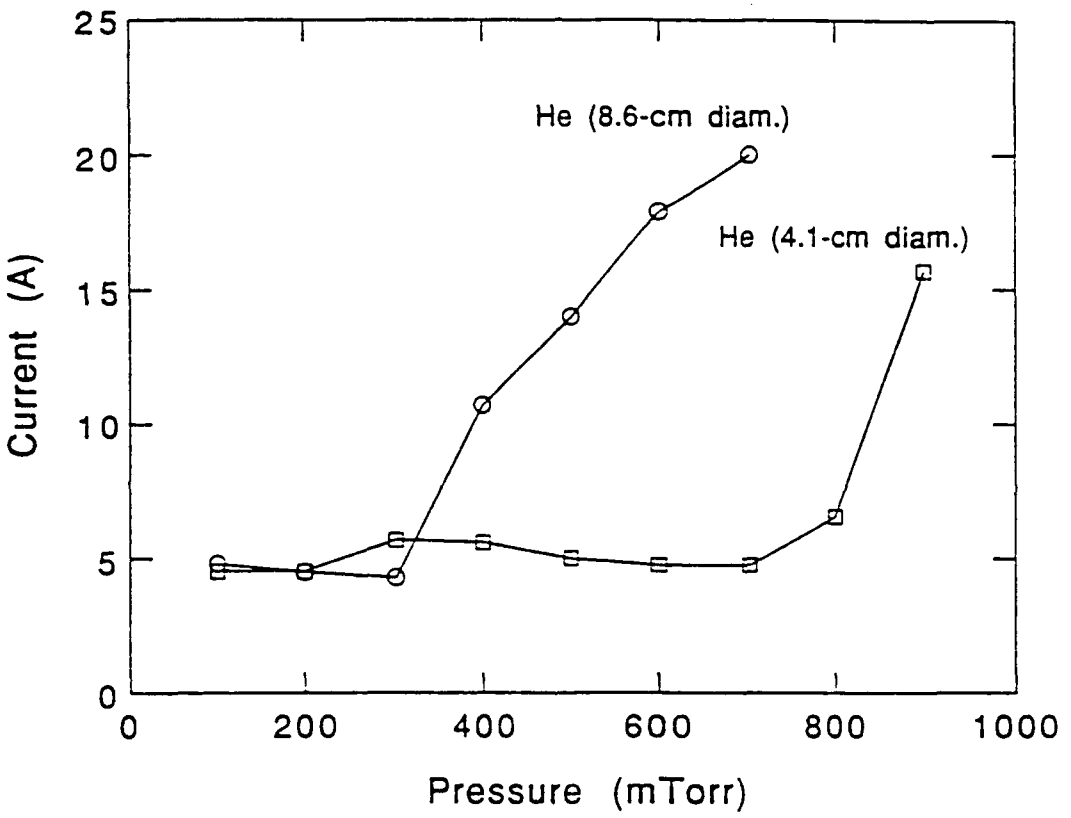

FIG. 5. Threshold discharge current dependence on the pressure.

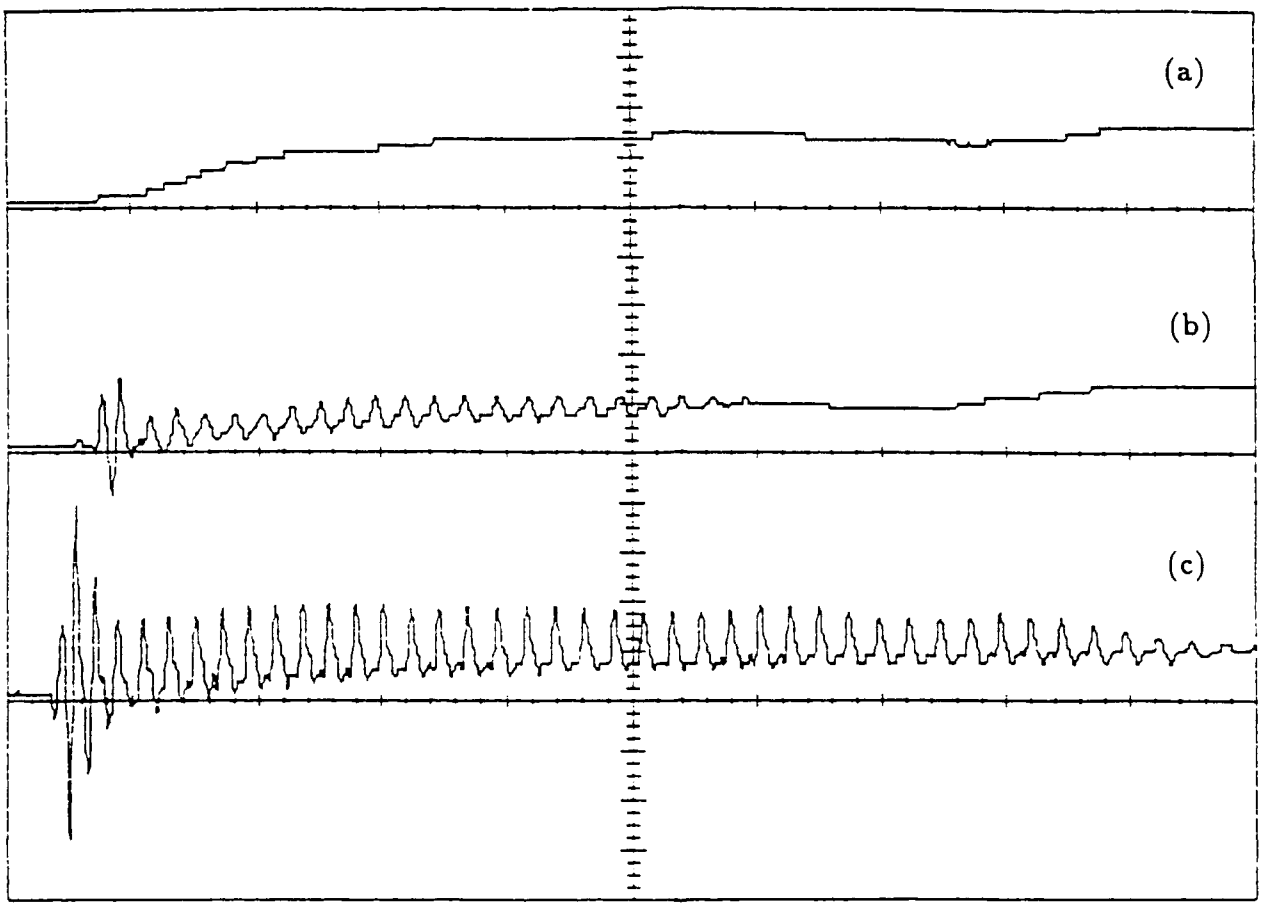

FIG. 6. Scope traces of electrostatic analyzer ion current. (a) without RF generation; (b) discharge current I_a slightly over threshold; (c) I_a well above threshold. Timebase 200 ns/div, sensitivity 10 mA/div.

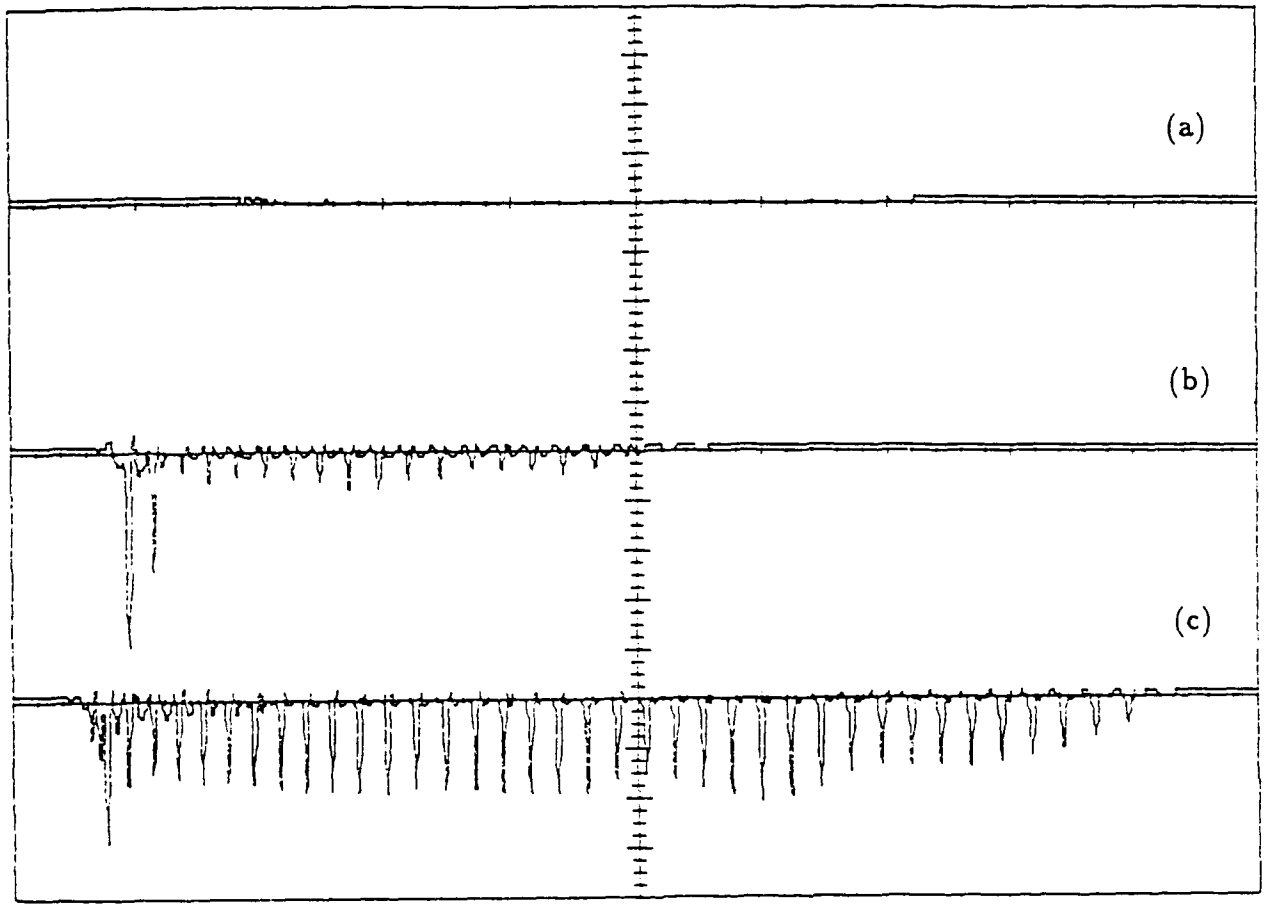

Fig. 7. Scope traces of electrostatic analyzer electron current. (a) without RF generation; (b) discharge current I_a slightly over threshold; (c) I_a well above threshold. Timebase 200 ns/div. Sensitivity is 10 mA/div for (a) and (b), and 20 mA/div for (c).

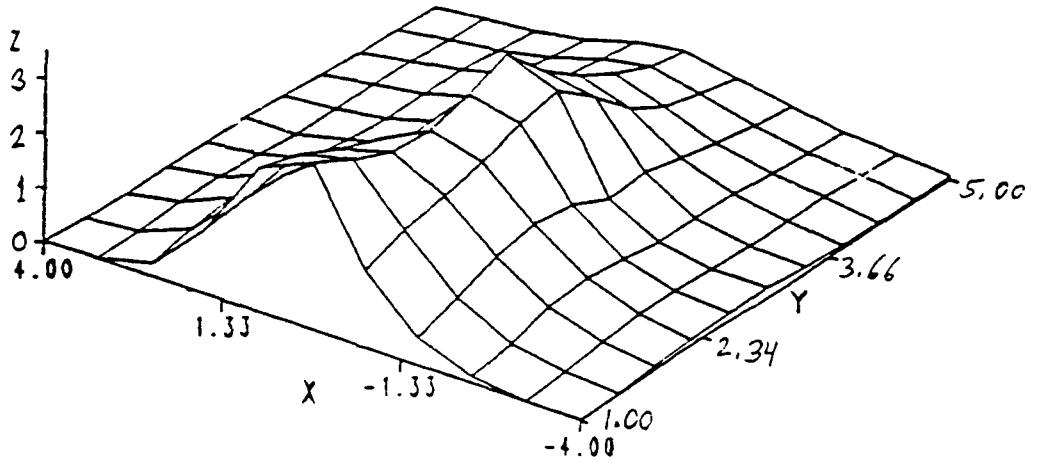

Fig. 8. Plasma density spatial distribution for the 8.6-cm-diam tube. x – radial distance from axis (in cm); y – axial distance from anode (in cm); z – density (in relative units). Gas was He with 120 mTorr pressure.

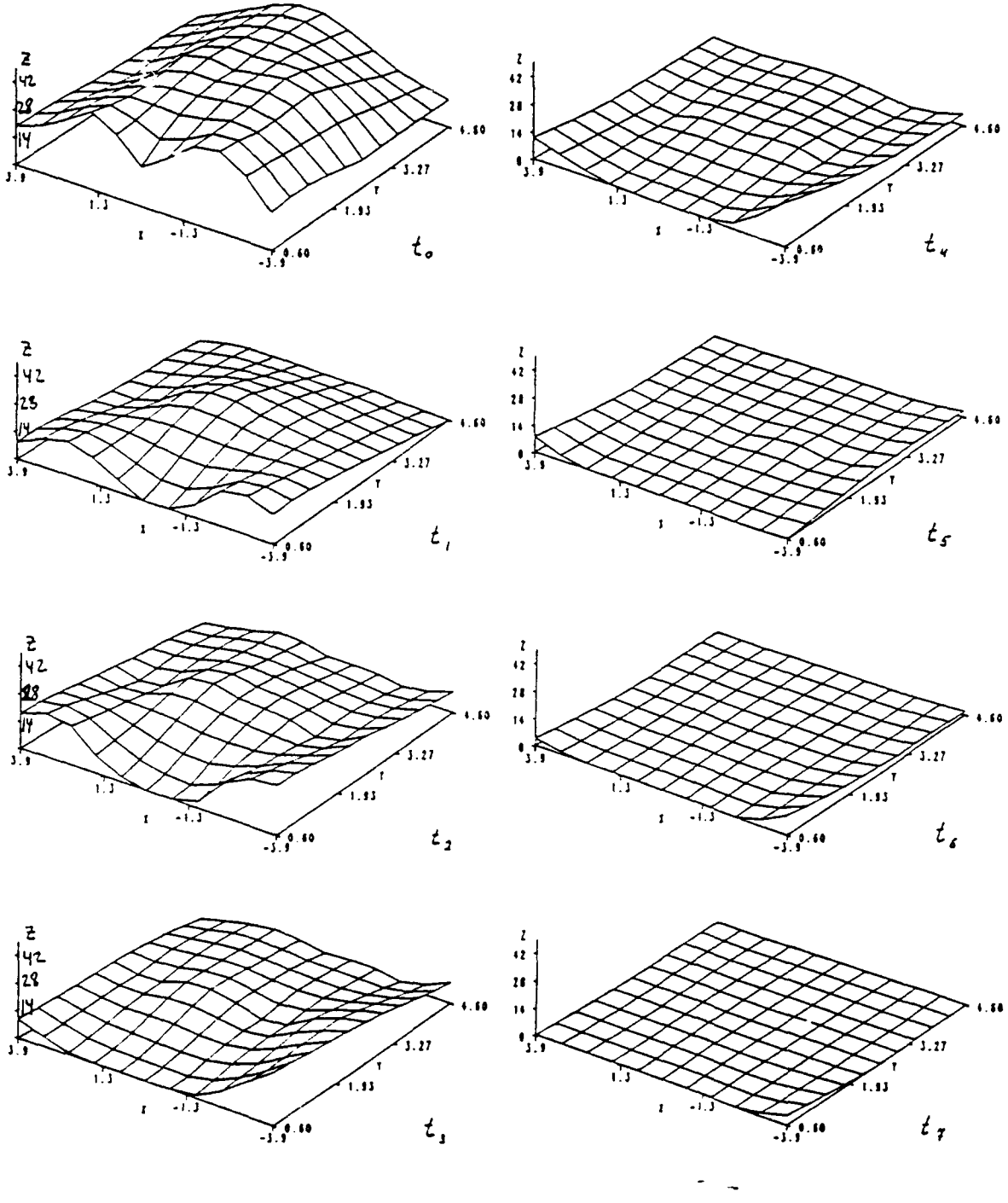

Fig. 9. Time evolution of spatial distribution of plasma waves for the 8.6-cm-diam tube. x – radial distance from axis (in cm); y – axial distance from anode (in cm); z – intensity (in relative units). t_0 is 250 ns from start of pulse. Δt is 250 ns. Gas was He with 120 mTorr pressure.

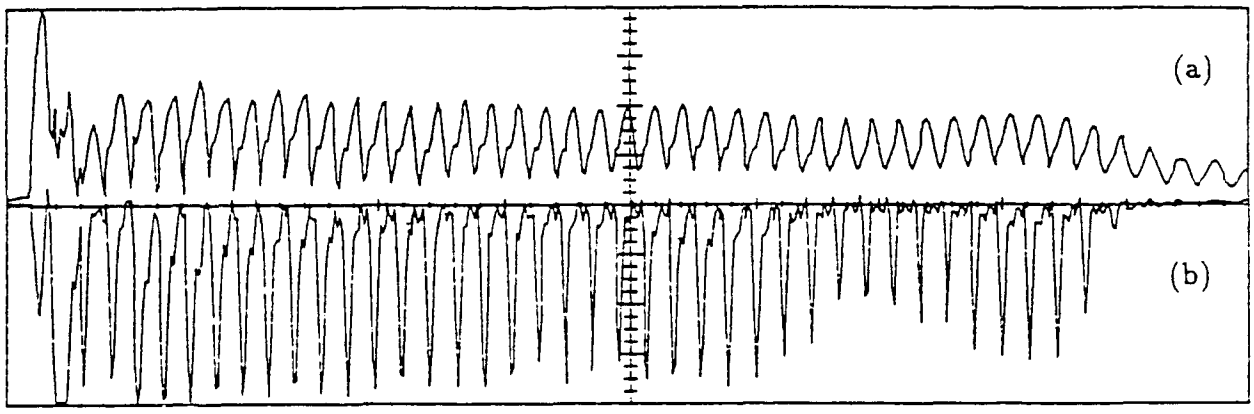

FIG. 10. Scope traces of: (a) the RF-modulated discharge current; (b) the detected microwave spikes. Timebase 200 ns/div. Sensitivity is 10 A/div for (a) and 10 mV/div for (b). Gas is He with 120 mTorr pressure.

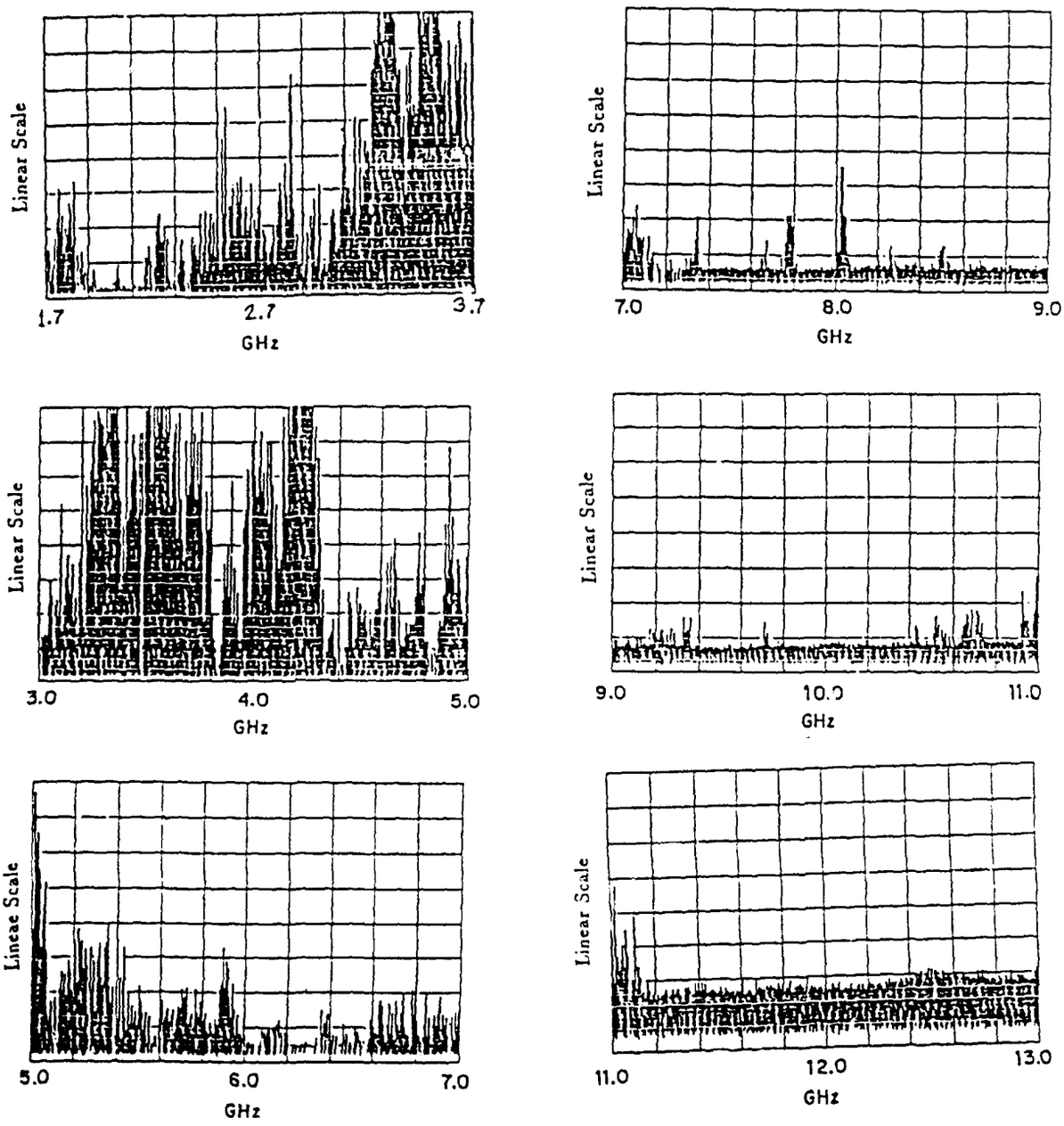

Fig. 11. Microwave spectrum from the 8.6-cm-diam tube. Gas is He with a pressure of 70 mTorr.

Bulletin of the American Physical Society
34th Annual Meeting of the APS Division of Plasma Physics
16-20 November 1992 - Seattle, WA

4R 26

ANALYSIS OF SOFT X-RAY SPECTRA FROM SHORT-PULSE LASER-PRODUCED PLASMAS THAT ARE CANDIDATES FOR A RECOMBINATION X-RAY LASER*--A.C. Abare, University of Florida, Gainesville; C.J. Keane, L. DaSilva, R.W. Lee, and M.D. Perry, Lawrence Livermore National Laboratory; R. Falcone, University of California, Berkeley-- We report on the analysis of streaked soft x-ray spectra obtained from the interaction of a short-pulse high-intensity laser (I_L~10^{17} W/cm^2) with neon gas targets. In these experiments long duration (~1 ns) line radiation from Li- and Be-like Ne is seen in addition to prompt harmonic emission. Transitions of the type 2s-np, 2p-nd, 3s-np, 3p-nd, and 3d-nf are identified. Line ratios and time histories are analyzed and compared with those obtained from simple modelling codes. The results are used to estimate the plasma conditions and determine if they are appropriate for producing late-time quasi-steady-state population inversions.

*Work performed under the auspices of the U.S. Department of Energy by Lawrence Livermore National Laboratory under contract W-7405-ENG-48.

4R 27

Radiation Electrodynamics of the Photo-electron Cloud Produced by an Arbitrary Photon Pulse Incident on a Planar Surface in Vacuum--Rigorous Results. DAVID DIETZ, Phillips Laboratory, High Energy Plasma Division (WSP), Kirtland AFB, NM 87117-6008. The electromagnetic radiation field produced by the cloud of accelerating electrons induced at a photoelectron emitting surface in vacuum by an arbitrary (in time) photon pulse incident upon that surface is derived analytically from first principles in the non-relativistic, small-spot-size regime. As a first step, non-relativistic electron cloud dynamics is presented; then integral expressions for the electric and magnetic fields at large but finite (i.e., "finitely-remote") distances from the cloud are derived. The fields are calculated by directly summing contributions over individual electron trajectories, using exact small-spot retarded times, rather than by the usual technique of first forming the electron current density and then integrating it. The resulting integral representations of the fields are correct to first order in v/c and are valid for all non-negative time and for somewhat long (in space) charge clouds. These finitely-remote fields are then used to compute asymptotic radiation fields and, subsequently, asymptotic radiation quantities in the limit of the field point going to infinity. Finally, an illustration of our results for a constant ("flat-top") pulse is presented.

X 4R 28 RF Oscillations and Microwave Generation in a Low-Pressure Hollow Cathode Discharge.* J. FELSTEINER, D. ARNEL, Z. BAR-LEV, A. ROSENBERG, AND YA. Z. SLUTSKER, Technion, Haifa, Israel. — Generation of high-intensity coherent RF oscillations close to the ion plasma frequency ($\omega \lesssim \omega_{pi}$) is observed in a low-pressure cylindrical hollow cathode discharge. Typical discharge parameters were: Cathode diameter 2 - 9 cm, gas pressure 0.05 - 1 Torr, current 5 - 100 A. Frequency observed was 20 - 70 MHz. This phenomenon is associated with instability of the cathode sheath which causes modulation of the discharge current of almost 100%. These intense RF oscillations are accompanied by short microwave spikes, each emitted at the same phase of the RF period. The microwave radiation has a wide spectrum above the electron plasma frequency ($\omega_{p_e} \lesssim \omega \lesssim 2\omega_{p_e}$). This radiation appears to be due to the transformation of electrostatic plasma waves which were measured inside the plasma and are assumed to be driven by the beam-plasma instability: The beam of primary electrons emitted from the cathode interacts with the discharge plasma. Both RF and microwave generation do not depend on the anode shape, area, or position (including the Orbitron geometry).

*Work supported in part by the U.S. AFOSR (Grant 88-0343).

SESSION 4S: POSTER SESSION: PARTICLE BEAMS AND ADVANCED ACCELERATORS

Tuesday afternoon, 17 November 1992
Fifth Avenue Room at 14:00

4S 1

Beam Extraction From a Stellatron Accelerator*, R. PROHASKA, Y. SONG, A. FISHER**, and N. ROSTOKER, University of California, Irvine -- The UCI stellatron has been redesigned for beam extraction. An electron ring with beam current of over 1 kA and energy of 11-12 MeV was produced in a graphite composite chamber by using plasma start-up. After the completion of acceleration, the beam orbit was expanded by a spiller field and the electrons were guided toward an extraction port by a kicker field. About 1200 nC of electron charge was guided into the port. The extracted electrons were lost quickly to the wall of the drift tube during the propagation through the structure. The loss was reduced by shielding the magnetic components transverse to the tube axis. About 100 nC of electrons traveled over 12 cm from the entrance of the extraction port. Detailed experimental results will be presented.

* Work supported by ONR.
**Naval Research Laboratory, Washington, DC.

4S 2 Identification of Toroidal Field Errors in a Modified Betatron Accelerator † P. LOSCHIALPO,[a] S.J. MARSH,[b] L.K. LEN,[c] T. SMITH,[c] and C.A. KAPETANAKOS[a] A newly developed probe has been used to detect errors in the toroidal magnetic field of the NRL modified betatron. Measurements indicate that the radial field components (errors) are 0.1 to 1% of the applied toroidal field. Such errors, in the typically 5 kG toroidal field, can excite resonances which drive the beam to the wall. Two sources of detected field errors are discussed. The first is due to the discrete nature of the twelve single turn coils which generate the toroidal field. Measurements and computer calculations indicate that it's amplitude varies from 0 to 0.2% as a function of radius. This error is a good suspect for causing the excitation of the damaging $\ell = 12$ resonance seen in our experiments. The other source of field error is due to the current feed gaps in the vertical magnetic field coils. A magnetic field is induced inside the vertical field coils' conductor in the opposite direction of the applied toroidal field. Fringe fields at the gaps lead to additional field errors which have been measured as large as 1.0%.

†Supported by ONR and SPAWAR, [a] Naval Research Laboratory, [b] SFA, Inc., [c] FM Technologies, Inc.

4S 3 Electron Beam-Breakup-Instability Growth Reduction Experiments Using External Coupled Cavities -- P.R. MENGE, R.M. GILGENBACH, M. WALTER, C.H. CHING and Y.Y. LAU, *Intense Energy Beam Interaction Laboratory, Nuclear Engineering Dept., University of Michigan, Ann Arbor, MI, 48109-2104.*—Experiments on electron beam transport through 10 RF cavities have shown that beam breakup (BBU) instability growth can be reduced by a factor of four when seven internal beam cavities are coupled by coaxial cable to seven external dummy cavities. The experiments are being performed with a long-pulse relativistic e-beam accelerator, MELBA, (t = 0.5 - 1.5 μs, V = ~0.7 - 0.8 MV, diode current = 1-15 kA, extracted current = 300 A, transported current = 200 A).The experiment consists of 10 brass pillbox resonant cavities immersed in a solenoidal field (1 - 4 kG). Each cavity contains a microwave coupling antenna positioned to be sensitive to the TM_{110} beam breakup mode which occurs at 2.5 GHz. The first cavity has its TM_{110} mode primed by a 1 kW microwave pulse (3 μs) from an external magnetron. Strong growth (~36 dB) of the 2.5 GHz RF measured between the 2nd and 10th cavities has been observed when a 200 A e-beam is injected into the uncoupled cavity system.[1] When seven internal cavities (3rd - 9th) are coupled to seven identical external dummy cavities via coaxial microwave cable, the 2.5 GHz RF growth is reduced to about 30 dB average.

1) P.R. Menge, R.M. Gilgenbach and R.A. Bosch, Appl. Phys. Lett., August, 1992

Supported by SDIO-IST through an ONR contract

Collision-induced resonant amplification of electromagnetic waves by electrons in circular orbits

J. Felsteiner and A. Rosenberg
Department of Physics, Technion-Israel Institute of Technology, 32000 Haifa, Israel

(Received 30 April 1990; accepted for publication 24 August 1990)

Electrons moving in circular orbits and colliding with gas atoms interact with a circular electromagnetic mode. Applying the linearized Boltzmann equation, the known nonresonant-stimulated bremsstrahlung and the near-resonance Landau effect are obtained. We predict that resonant electrons moving with angular velocity equal to the azimuthal phase velocity of the electromagnetic wave can exchange energy with the wave if the momentum transfer cross section for an electron-atom collision is velocity dependent. Amplification is obtained if the momentum transfer cross section has a positive slope.

I. INTRODUCTION

Electrons encircling positive electrodes had been applied for producing microwaves in a device called a Heliotron.[1] Two decades later, Alexeff and Dyer introduced the gas Orbitron.[2] This device is based on a glow discharge produced between a hollow cylindrical cathode and a positive wire anode. The success of the gas Orbitron stimulated research on the vacuum Orbitron.[3] However, results obtained by other groups[4,5] raised a debate as to whether the microwave emission of the gas Orbitron is due to the Orbitron mechanism suggested in Ref. 2. Schumacher and Harvey[4] claimed that the observed radiation is consistent with the generation by nonlinear wave-wave coupling of counter-streaming electron plasma waves. Our group[5] suggested that the gas Orbitron, which basically is a glow-discharge tube, radiates microwaves by the same mechanism responsible for the amplification of millimeter waves observed in the negative glow of a glow-discharge tube.[6] This amplification was explained as stimulated emission of bremsstrahlung in electron-atom collisions, enhanced by the multicollision effect.[7]

Recently Ben-Aryeh and Postan[8] tried a unified model, including both the electron-orbit effect and the influence of collisions. They assumed electrons moving in circular orbits, interacting with a circular electromagnetic mode, and colliding with the background gas atoms. The linearized Boltzmann equation was applied for a specific distribution and their results led to the following conclusion: The inverse Landau damping and the stimulated bremsstrahlung induced by the collisions are operating in opposite directions to each other and tend to have a compensating effect on the amplification process. They claim that the inverse Landau damping is the dominant effect in the Orbitron maser.

Although the assumption of a thin annulus of electrons moving in circular orbits is not appropriate for the glow-discharge gas Orbitron, one can consider a device in which such an electron distribution is produced and a controlled amount of gas is added to effect electron-atom collisions. In this paper, the influence of these collisions on the amplification (absorption) of electromagnetic waves in such a device is theoretically investigated. The linearized Boltzmann equation is applied, but instead of trying a specific distribution (as was done in Ref. 8), a quite general approach will be taken. The results derived in the following sections are different from those of Ben-Aryeh and Postan[8] and can be summarized as follows:

(a) Far from resonance (or without resonance for TE_{0n} modes), the known expressions of (single-collision) stimulated bremsstrahlung theory[6] are obtained.

(b) Near resonance the (inverse) Landau damping is dominant for TE_{ln} modes with $l \neq 0$. The collisions reduce both amplification and absorption of the electromagnetic wave caused by the (inverse) Landau damping effect.

(c) At resonance, amplification effected by electron-atom collisions is predicted. The conditions necessary for amplification are similar to those reported by Wachtel and Hirshfield[9] for electrons at the cyclotron resonance in a magnetic field.

II. THEORETICAL MODEL

Following Ref. 8 we start with the linearized Boltzmann equation:

$$\frac{\partial f_1}{\partial t} + \mathbf{v}\cdot\frac{\partial f_1}{\partial \mathbf{r}} - \frac{e}{m}\mathbf{E}\cdot\frac{\partial f_0}{\partial \mathbf{v}} = -\nu f_1, \tag{1}$$

where $f_0(\mathbf{v})$ is the electron distribution in the absence of the rf field perturbation, $f_1(\mathbf{v},t)$ is a small perturbation caused by the electromagnetic wave with electric vector $\mathbf{E}$, and $\nu(\mathbf{v})$ is the velocity-dependent collision frequency. Assuming that the electrons are moving in a circle of radius r with angular velocity ω_0, then

$$\mathbf{v} = \omega_0 r\hat{\theta}, \quad f_0(\mathbf{v}) = f_0(\omega_0),$$

and

$$\frac{\partial f_0}{\partial \mathbf{v}} = \frac{1}{r}\frac{\partial f_0}{\partial \omega_0}\hat{\theta},$$

so that Eq. (1) becomes

$$\frac{\partial f_1}{\partial t} + \omega_0\frac{\partial f_1}{\partial \theta} - \frac{eE_\theta}{mr}\frac{\partial f_0}{\partial \omega_0} = -\nu(\omega_0)f_1. \tag{2}$$

In a cylindrical (or coaxial) geometry, electromagnetic modes with $E_\theta \neq 0$ can propagate, namely, TE_{ln} ($l = 0,1,2,\ldots$) and TM_{ln} ($l = 1,2,\ldots$). For these modes the time and angular dependence of E_θ is

 0021-8979/90/245981-04$03.00

$E_\theta \sim e^{-i(\omega t - l\theta)}$.

Therefore, f_1 should also have this dependence, and we obtain from Eq. (2):

$$f_1 = \frac{-i(e/mr)}{(l\omega_0 - \omega) - i\nu} \frac{\partial f_0}{\partial \omega_0} E_\theta. \tag{3}$$

The perturbed azimuthal current density J_θ is obtained from f_1:

$$J_\theta = -en_e r^2 \int_{-\infty}^{+\infty} \omega_0 f_1(\omega_0) d\omega_0, \tag{4}$$

where n_e is the electron density. Using Eqs. (3) and (4) the rf conductivity, defined as $\sigma = J_\theta / E_\theta$, is calculated:

$$\sigma = i\left(\frac{e^2 n_e r}{m}\right) \int_{-\infty}^{+\infty} \frac{\omega_0}{(l\omega_0 - \omega) - i\nu} \frac{\partial f_0}{\partial \omega_0} d\omega_0. \tag{5}$$

For $\omega_0 < 0$ there is no resonance ($l\omega_0 - \omega \neq 0$), therefore, we shall consider only $\omega_0 > 0$, that is, electrons rotating in the same direction as the electromagnetic wave. The integration in Eq. (5) will be limited to $\int_0^\infty d\omega_0$.

The amplification/absorption of the electromagnetic wave is proportional to the real part of the rf conductivity σ as follows:

For $\mathrm{Re}\{\sigma\} > 0$, absorption.

For $\mathrm{Re}\{\sigma\} < 0$, amplification.

Since the effect of collisions is investigated, $\nu \neq 0$, and the integrand in Eq. (5) is finite, provided $\partial f_0 / \partial \omega_0$ is finite (as should be for a physically possible distribution). This allows us to separate the real part of σ in Eq. (5):

$$\mathrm{Re}\{\sigma\} = -\left(\frac{e^2 n_e r}{m}\right) \int_0^\infty \frac{\omega_0 \nu}{(l\omega_0 - \omega)^2 + \nu^2} \frac{\partial f_0}{\partial \omega_0} d\omega_0. \tag{6}$$

Obviously, if $\partial f_0 / \partial \omega_0 < 0$ for $0 < \omega_0 < \infty$, $\mathrm{Re}\{\sigma\} > 0$, and *no* amplification can be obtained. For example, absorption of the electromagnetic wave is predicted for a Maxwellian distribution. From Eq. (6) we see that the sign of $\mathrm{Re}\{\sigma\}$ is fixed by the integral of $\partial f_0 / \partial \omega_0$ over the whole range where

$$\frac{\omega_0 \nu}{(l\omega_0 - \omega)^2 + \nu^2} \neq 0,$$

and it should be noted that for any physical distribution, a region with $\partial f_0 / \partial \omega_0 > 0$ is followed by a region where $\partial f_0 / \partial \omega_0 < 0$.

A much clearer physical picture is obtained if the integration is done on $f_0(\omega_0)$. Then one can calculate the contribution of electrons with velocity ω_0 to amplification/absorption, and conclude which distribution $f_0(\omega_0)$ is optimal for obtaining amplification. Integration by parts of Eq. (6) yields

$$\mathrm{Re}\{\sigma\} = \left(\frac{e^2 n_e r}{m}\right) \int_0^\infty f_0(\omega_0) \times \frac{\partial}{\partial \omega_0} \left(\frac{\omega_0 \nu}{(l\omega_0 - \omega)^2 + \nu^2}\right) d\omega_0. \tag{7}$$

The collision frequency ν is obtained from the momentum transfer cross section σ_M:

$$\nu = v n_a \sigma_M(v) = r\omega_0 n_a \sigma_M(\omega_0), \tag{8}$$

where n_a is the atom density. σ_M is the experimentally measured quantity generally given for electron-atom scattering (rather than ν). A straightforward evaluation of the derivative in Eq. (7), together with Eq. (8), enables us to express $\mathrm{Re}\{\sigma\}$ in terms of σ_M and $\partial \sigma_M / \partial \omega_0$ as follows:

$$\mathrm{Re}\{\sigma\} = -\left(\frac{e^2 n_e n_a r^2}{m}\right) \int_0^\infty f_0(\omega_0) G(\omega_0) d\omega_0, \tag{9}$$

where

$$G(\omega_0) = -\omega_0 \frac{\omega_0 (\partial \sigma_M / \partial \omega_0)[(l\omega_0 - \omega)^2 - \nu^2] - 2\omega\sigma_M(l\omega_0 - \omega)}{[(l\omega_0 - \omega)^2 + \nu^2]^2}. \tag{10}$$

The amplification of electrons with angular velocity ω_0 is proportional to $G(\omega_0)$ [absorption for $G(\omega_0) < 0$]. Given the parameters of the electromagnetic wave (ω and l) and the type of gas (for which σ_M is known), the gain function $G(\omega_0)$ can be calculated. Then, for *any* distribution $f_0(\omega_0)$ the net gain (or attenuation) can be evaluated. It should be noted that Eqs. (9) and (10) were derived for electrons moving in circular orbits, from the linearized Boltzmann equation, without any approximations.

III. APPLICATIONS

In order to demonstrate the physical content of the equations derived above, the following regions will be analyzed further: Nonresonant interaction, near-resonance interaction, and at-resonance interaction.

A. Nonresonant stimulated bremsstrahlung

The Boltzmann equation was applied by Bekefi[10] to calculate the amplification of a plane wave by stimulated bremsstrahlung in electron-atom (ion) collisions. For low collision rates, $\nu \ll \omega$, the results are identical to those obtained later by other methods.[6] The nonresonant conditions are $(l\omega_0 - \omega)^2 \gg \nu^2$ or $l = 0$. For $l = 0$ the electromagnetic mode is TE_{0n}, for which the electric field E_θ is independent of θ. Therefore, electrons moving in circular orbits, parallel to the electric-field vector, should contribute to amplification as do electrons moving in the direction of the electric field vector of a plane wave. From Eq. (10), for $l = 0$ and $\omega^2 \gg \nu^2$ we obtain

$$G(\omega_0) \cong -\frac{\omega_0}{\omega^2} \left(\omega_0 \frac{\partial \sigma_M}{\partial \omega_0} + 2\sigma_M\right). \tag{11}$$

For comparison with the results of Ref. 6, we transform Eq. (11) to the energy variable ϵ, defined by

$$\epsilon = \tfrac{1}{2} m r^2 \omega_0^2. \tag{12}$$

Then the amplification of electrons with energy ϵ is proportional to

$$G(\epsilon) \sim -\epsilon^{1/2}\left(\epsilon \frac{\partial \sigma_M}{\partial \epsilon} + \sigma_M\right). \quad (13)$$

This equation is identical to the one obtained in Ref. 6 for electrons moving in the direction of the electric vector of the electromagnetic wave. Note that negative $\partial\sigma_M/\partial\epsilon$ is a necessary condition for obtaining amplification.

B. Near-resonance interaction

The resonance is obtained when $l\omega_0 - \omega = 0$. Then the electrons are moving with angular velocity equal to the azimuthal phase velocity of the electromagnetic wave. Assume that the distribution $f_0(\omega_0)$ is peaked near a resonance. We define the condition of near resonance by

$$(l\omega_0 - \omega)^2 \ll \nu^2. \quad (14)$$

The gain function of Eq. (10) with the above approximation is

$$G(\omega_0) \approx \frac{2\omega_0\omega}{\nu^4}\sigma_M(l\omega_0 - \omega) + \frac{\omega_0^2}{\nu^2}\frac{\partial\sigma_M}{\partial\omega_0}. \quad (15)$$

The first term of Eq. (15) is zero at exact resonance, positive above resonance, and negative below resonance. It can be physically identified with the inverse Landau damping effect: Electrons moving with (angular) velocity ω_0 larger than the (azimuthal) phase velocity of the electromagnetic wave ω/l, make $l\omega_0 - \omega > 0$, and amplify the electromagnetic wave, and vice versa, electrons slower than the phase velocity absorb energy from the electromagnetic wave.

The effect of collisions on the Landau effect is obvious in the first term of Eq. (15): Both the Landau and the inverse Landau effects are attenuated strongly by the collisions. Since $\nu \sim \omega_0\sigma_M$, the (inverse) Landau effect is proportional to ν^{-3}. Note that Eq. (15) is exact only near the resonance. If $(l\omega_0 - \omega)^2$ is larger than ν^2, Eq. (10) should be used.

C. At-resonance interaction

At resonance the first term of Eq. (15) goes to zero, and the gain function $G(\omega_0)$ can be approximated as

$$G(\omega_0) \approx \frac{\omega_0^2}{\nu^2}\frac{\partial\sigma_M}{\partial\omega_0}. \quad (16)$$

Thus, at resonance, amplification is obtained if $\partial\sigma_M/\partial\omega_0 > 0$. Negative slope σ_M exists in the noble gases Ne, Ar, Xe, Kr, for electrons with energies of few eV, due to the Ramsauer effect.

The resonant interaction expressed by Eq. (16) is similar to the effect reported by Wachtel and Hirshfield.[9] They predicted theoretically and found experimentally that electrons within a xenon gas, with energies of few eV, amplify an electromagnetic wave at a frequency equal to the cyclotron frequency of the electrons in the applied magnetic field.

D. Effect of the electron distribution

The gain expected from each type of interaction depends on the electron distribution, gas type, and pressure. The nonresonant stimulated bremsstrahlung is effective with broad electron distributions, provided most of the electrons have energies in the range where $\epsilon\partial\sigma_M/\partial\epsilon + \sigma_M < 0$, as is evident from Eq. (13).

The near-resonance Landau interaction is operative in most microwave devices. An initial mistune is necessary for obtaining gain, namely, the optimal electron distribution is a narrow one, peaked at ω_0 slightly larger than ω/l, as can be seen in Eq. (15). The collisions with gas atoms have a detrimental effect on the amplification.

The resonant collision-induced gain is maximal for an initial δ distribution at the exact resonance ($l\omega_0 - \omega = 0$). However, for real distributions, the mistune Landau effect will accompany the collision-induced effect. To compare the effects, we calculate by Eq. (15) the ratio between the mistune gain G_M and the resonant collision-induced gain G_C as follows:

$$\frac{G_M}{G_C} = \frac{2\omega_0\omega\sigma_M(l\omega_0 - \omega)}{\nu^2\omega_0^2(\partial\sigma_M/\partial\omega_0)} = \left(\frac{\sigma_M}{\epsilon(\partial\sigma_M/\partial\epsilon)}\right)\frac{\omega(l\omega_0 - \omega)}{\nu^2}. \quad (17)$$

The term in large parentheses can be evaluated from standard atomic data.[11] For electrons of about 8 eV, colliding with argon atoms, it is approximately equal to one. Near the resonance ω can be replaced by $l\omega_0$. The collision frequency ν, given by Eq. (8), can be controlled by the gas pressure. However, ν must be limited to comply with the basic assumption that the electrons are moving in circular orbits. We limit ν by requiring that an electron will make (on the average) at least one complete revolution, i.e., $\nu < \omega_0/2\pi$, so that

$$\frac{G_M}{G_C} \cong \frac{l\omega_0(l\omega_0 - \omega)}{(\omega_0/2\pi)^2} = (2\pi l)^2\frac{(\omega_0 - \omega/l)}{\omega_0}. \quad (18)$$

The condition $G_M \cong G_C$ is obtained when the normalized deviation from resonance $(\omega_0 - \omega/l)/\omega_0$ equals $1/(2\pi l)^2$. For $l = 1$ it is $\pm 2.5\%$. Thus, the resonant collision-induced gain will dominate if the electron distribution has a 5% width and centered at resonance.

The evaluation of efficiencies should be done on the basis of a nonlinear model. From the present linear model we identify the difficulty of maintaining a 5%-wide distribution in the presence of collisions. The main nonlinear effect expected is a collision-induced production of bunching in the electrons which are initially distributed with random phases with respect to the electromagnetic wave. This bunching should enhance the gain.

IV. DISCUSSION

There is an interesting difference between the nonresonant and at-resonance effects of the collisions on the interaction: Negative $\partial\sigma_M/\partial\omega_0$ is necessary for amplification in the first case, while a positive $\partial\sigma_M/\partial\omega_0$ is required for the second. This is a manifestation of the different physical processes involved. In the nonresonant conditions the energy exchange between the electrons and the electromagnetic wave is enabled by the collisions, in the process called "stimulated bremsstrahlung." Here the atoms provide the necessary momentum for the emission (absorption) of photons

by the electrons. On the other hand, at resonance the required momentum is supplied by the external force which drives the electrons in the circular orbits. Here the role of collisions can be explained as follows: For $l\omega_0 = \omega$ the electrons are rotating with angular velocity equal to the azimuthal phase velocity of the electromagnetic wave. Half of the electrons are accelerated and half are decelarated by the electric field of the wave, so that there is no net transfer of energy. However, if $\partial\sigma_M/\partial\omega_0 > 0$, those electrons which have absorbed energy from the wave, have a greater velocity, therefore a greater probability of being knocked out of the circular orbit than those which lose energy to the electromagnetic wave and become slower. The result is a net transfer of energy from the electrons to the electromagnetic wave, i.e., amplification.

In view of the above, the resonant processes are not "stimulated bremsstrahlung" although they are effected by the collisions. The near-resonance Landau effect was obtained for a specific distribution by Ben-Aryeh and Postan.[8] However they seem to have misinterpreted their result [Eq. (11) of Ref. 8], namely, it is not the "stimulated bremsstrahlung" which opposes the Landau effect, but rather the attenuation of the Landau effect caused by collisions, as expressed quite generally in Eq. (15). Note also that the electron-radiation interaction is zero for $l\omega_0 = \omega$, according to Eq. (11) of Ref. 8. The resonant effect of Eq. (16) seems to have been lost in the approximations of Ref. 8.

The theoretical results derived above cannot explain the microwave emission of the gas Orbitron, since the required distribution is not supposed to exist in a gas discharge. The electron distribution is broad and not peaked as necessary for the resonant interactions. However, the multicollision-enhanced stimulated bremsstrahlung[7] can support nonresonant amplification of electromagnetic waves.

The results presented in this paper should be tested in a vacuum Orbitron (or Heliotron), to which a controlled amount of gas has been added. The main problem expected in such an experiment is that too high gas pressure might destroy the needed electron distribution, while with too low gas pressure the effects of the collisions might be negligible.

ACKNOWLEDGMENT

This work was supported in part by the U.S. Air Force Office of Scientific Research under Grant No. AFOSR-88-0343.

[1] D. A. Watkins and G. Wada, Proc. IRE 46, 1700 (1958).
[2] I. Alexeff and F. Dyer, Phys. Rev. Lett. 45, 351 (1980).
[3] J. M. Burke, W. M. Manheimer, and E. Ott, Phys. Rev. Lett. 56, 2625 (1986); A. K. Ganguly, H. P. Freund, and S. Ahn, Phys. Rev. A 36, 2199 (1987).
[4] R. W. Schumacher and R. J. Harvey, *1984 IEEE International Conference on Plasma Science* (IEEE, New York, 1984), p. 109; Bull. Am. Phys. Soc. 29, 1179 (1984).
[5] J. Felsteiner, A. Rosenberg, D. Arbel, and J. Politch, Int. J. Infrared Millimeter Waves 8, 479 (1987).
[6] A. Rosenberg, Y. Ben-Aryeh, J. Politch, and J. Felsteiner, Phys. Rev. A 25, 1160 (1982).
[7] A. Rosenberg, Y. Ben-Aryeh, J. Felsteiner, and J. Politch, Phys. Rev. Lett. 49, 1917 (1982).
[8] Y. Ben-Aryeh and A. Postan, Opt. Commun. 73, 304 (1989).
[9] J. M. Wachtel and J. L. Hirshfield, Phys. Rev. Lett. 19, 293 (1967).
[10] G. Bekefi, "Bremsstrahlung Instability in a Plasma Induced by Electron Streaming," M.I.T. Quarterly Progress Report No. 104 (1972).
[11] See, e.g., M. Mitchner and C. H. Kruger, Jr., *Partially Ionized Gases* (Wiley, New York, 1973).